Isı Bilimi ve Tekniği Dergisi, 41, 1, 101-118, 2021
J. of Thermal Science and Technology

ISSN 1300-3615
https://doi.org/10.47480/isibted.979363

A COMPARATIVE STUDY OF DIFFUSION, THERMAL WAVE AND DUAL-PHASE-LAG HEAT CONDUCTION IN THIN LAYER

R. YUVARAJ* and D. SENTHILKUMAR**
*Assistant Professor, Mechanical Engineering, Sona College of Technology, Salem - 636005, India
yuvarajr@sonatech.ac.in, ORCID: 0000-0002-5322-6084
**Professor and Head, Mechanical Engineering, Sona College of Technology, Salem - 636005, India
senthilkumard@sonatech.ac.in, ORCID: 0000-0001-9538-100X

(Geliş Tarihi: 09.04.2020, Kabul Tarihi: 05.02.2021)

Abstract: In the present work, three different modes of heat conduction, diffusion, thermal wave, and dual-phase lag, across a thin layer subjected to a constant temperature and insulated boundary conditions are compared by using a finite element solution. The finite element model is developed by considering relaxation time to heat flux and relaxation time to temperature gradient for a single element. After assembling all the elements, the number of algebraic equations obtained is solved to predict the temperature distribution across the thin layer using Python. The solution predicted by the dual-phase lag is compared with that obtained by the single-phase Cattaneo–Vernotte's model and diffusion Fourier model. The developed model is validated with analytical, numerical, and experimental solutions with good agreement. The temperature contours are plotted for all three conditions and the way it propagates differently through the thin layer is clearly shown. Further, the temperature variation at the center of the layer, at which collision occurred, is predicted and the speed of the thermal wave, infinite in the Fourier diffusion model and finite in both single and dual-phase lag, is examined under transient to steady-state condition.
Keywords: dual-phase lag, CV model, relaxation time, finite element model, python.

İNCE TABAKADA DİFÜZYON, TERMAL DALGA VE ÇİFT FAZLI-LAG ISI İLETİMİNİN KARŞILAŞTIRMALI BİR ÇALIŞMASI

Özet: Bu çalışmada, sabit bir sıcaklığa ve yalıtılmış sınır koşullarına maruz kalan ince bir katman boyunca üç farklı ısı iletimi, difüzyon, termal dalga ve çift fazlı gecikme modu, sonlu bir eleman çözümü kullanılarak karşılaştırılmıştır. Sonlu eleman modeli, tek bir eleman için akıyı ısıtmak için gevşeme süresi ve sıcaklık gradyanı için gevşeme süresi dikkate alınarak geliştirilmiştir. Tüm elemanları birleştirdikten sonra, elde edilen cebirsel denklemlerin sayısı Python kullanılarak ince katman boyunca sıcaklık dağılımını tahmin etmek için çözülür. Çift fazlı gecikme ile tahmin edilen çözüm, tek fazlı Cattaneo – Vernotte modeli ve difüzyon Fourier modeli ile elde edilen çözüm ile karşılaştırılır. Geliştirilen model, analitik, sayısal ve deneysel çözümlerle iyi bir uyum içinde doğrulanmıştır. Her üç koşul için sıcaklık sınırları çizilmiştir ve ince katman boyunca farklı şekilde yayılma şekli açıkça gösterilmiştir. Ayrıca, çarpışmanın meydana geldiği katmanın merkezindeki sıcaklık değişimi tahmin edilir ve Fourier difüzyon modelinde sonsuz ve hem tek hem de çift fazlı gecikmede sonlu olan termal dalganın hızı, geçici olarak kararlı durum koşulu.
Anahtar Kelimeler: çift fazlı gecikme, CV modeli, gevşeme süresi, sonlu eleman modeli, python.

NOMENCLATURE

Symbols

q	heat flux [W/m^2]
k	thermal conductivity [W/m·K]
T	temperature [K]
∇T	temperature gradient [K/m]
t	time [s]
L	thickness of the layer [m]
c_p	specific heat capacity [J/kg·K]
l	element length [m]
Z	dimensionless relaxation time
$[M]$	mass matrix
$[C]$	capacitance matrix
$[K]$	stiffness matrix
$\{F\}$	force vector

Greek Symbols

τ	relaxation time [s]
ρ	density [kg/m^3]
α	thermal diffusivity [m^2/s]
ξ	dimensionless distance
η	dimensionless time
θ	dimensionless temperature
ζ	dimensionless heat flux

Subscripts

q	heat flux
T	temperature gradient

INTRODUCTION

The synthesis of thin coatings is of great interest to engineers and physicists in modern technology. The energy transfer takes place over extremely small dimensions and time scales like etching of printed circuits, thin-film superconductors, fins, reactor walls, the satellite in orbit, thermal barrier coatings used in gas turbines, heating and cooling of micro-electronic elements involving a duration time of nanosecond or even picosecond in which energy is absorbed within a distance of microns from the surface. It is always required a correct prediction of thermal behavior to avoid thermal damage in devices. A major factor that depicts the energy transfer of the above applications requires certain non-Fourier conduction effects that need to be taken into account for the accurate prediction of heat transfer across thin layers.

The Fourier diffusive mode of heat conduction, parabolic in nature,

$$q = -k\,\nabla T \tag{1}$$

is accurate and appropriate in most common engineering situations for solving heat conduction problems. The most important drawbacks of the Fourier heat conduction model for solids are the prediction of thermal wave propagation speed and the simultaneous development of heat flux and temperature gradient. The rise of electron temperature is much faster than that of the lattice because of the faster interaction between the photons and electrons when large energy fluxes are deposited onto a metallic substrate in the form of electromagnetic radiation and the distinct relaxation time activates the electrons ballistically (Qui and Tien, 1992). Moreover, finite relaxation time is required for local thermal equilibrium to be established between the electrons and photons. The infinite speed of thermal wave leads to inaccurate results in situations where short-time inertial effects are dominant. Thus, Cattaneo (1958) and Vernotee (1958) proposed the thermal wave (CV) model,

$$\tau\frac{\partial q}{\partial t} + q = -k\,\nabla T \tag{2}$$

to consider a finite speed of thermal propagation by considering relaxation time τ. Tan and Yang (1997) investigated the propagation of the thermal wave in thin films subjected to sudden temperature changes on its surfaces. This investigation was extended to study the asymmetrical temperature changes on both sides (Tan and Yang, 1997). Li *et al.* (2005) developed an implicit difference scheme by considering the non-Fourier conduction effects in multilayer materials for rapid transient heat conduction under pulsed heating. Torii and Yang (2205) examined the heat transfer mechanism in a thin layer with symmetrical heat source impingement on its boundaries. Lewandowska and Malinowski (2006) presented an analytical solution of the hyperbolic heat conduction equation for the case of a thin slab symmetrically heated on both sides. Mitra *et al.* (1995) presented experimental evidence of hyperbolic heat transfer in processed meat for different conditions and experimentally determined the relaxation time for processed meat. Lam and Fong (2011) considered the effect of thermal diffusion and wave propagation in solids subjected to a time-varying and spatially decaying laser irradiation and the temperature profiles. Further, this study examined the temperature across the thin film subjected to asymmetrical boundary conditions by solving the CV model with non-homogeneous boundary conditions with the superposition principle (Fong and Lam, 2014).

The relaxation time τ in Eq. (2) is the phase lag between the heat flux and the temperature gradient. When $\tau = 0$, Eq. (2) reduces to the classical Fourier equation and τ is small, Eq. (2) reduces to the exponential relaxation model. The CV model does not account for the finite thermal relaxation time for the electrons and lattice to reach local thermal equilibrium. A two-step model for phonon-electron interaction has been proposed to account for the microscale response of thin metallic films subjected to short-pulse laser heating (Fujimoto *et al.*, 1984; Elsayed-Ali, 1991; Hector *et al.*, 1992; Majumdar, 1993). Korner and Bergman (1998) found that the hyperbolic approach to the heat current density violates the fundamental law of energy conservation and the solution obtained by the CV model is physically impossible solutions with negative local heat content. Tzou (1995; 1996) proposed a dual-phase lag (DPL) model,

$$\tau_q\frac{\partial q}{\partial t} + q = -k\,\nabla T - k\tau_T\frac{\partial}{\partial t}(\nabla T) \tag{3}$$

where τ_q and τ_T are the phase lags for the heat flux and the spatial temperature gradient concerning the local temperature, which is capable of predicting both the observed microscale and macroscale effects in conduction and found that the wave model overestimates the peak value of transient temperatures and the DPL model accurately describes the entire transient response. In fact, τ_q is related to the thermal wave speed and τ_q represents the time constant for electron-phonon equilibrium. When $\tau_q = 0$ and $\tau_T = 0$ the Eq. (3) reduces to classical Fourier equation, and $\tau_T = 0$ Eq. (3) reduces to CV model. Antaki (1998) used the DPL model to study the microscale transient heat conduction in a semi finite slab with surface flux. Tang and Araki (2000) solved the DPL model analytically to analyze the transient heat conduction in a finite medium subjected to pulse surface heating. Al-Nimr and Al-Huniti (2000) used the DPL model to explore the transient thermal stresses induced by rapid heating in a thin plate. Siva Prakash *et al.* (2000) identified the origin of the discrepancy in the available analytical results as the sensitivity of the predicted solution to the way of implementing the surface boundary condition. Also employed finite element method and fourth-order Runge–Kutta time marching procedure for the prediction

of spatial and temporal discretization, respectively. Liu and Cheng (2006) investigated heat conduction induced by a pulsed volumetric source in a two-layered film with the dual-phase-lag model. An analytical method and a numerical scheme are used to solve the DPL problem. Recently, Dhanaraj *et al.* (2019) resolved the DPL heat conduction using a three-time level finite difference scheme in a micro-scale gold film subjected to spontaneous temperature boundary conditions without knowing the heat flux. Tang *et al.* (2007) employed the dual-phase-lagging model (DPL), including the thermal wave situation, to simulate the temperature responses of the specimens and shown the absence of temperature jump caused by thermal wave propagation by comparing with the experimental results. Also found a wave-like shape predicted by the DPL model, which is almost the same as the numerical results from the Fourier model for heterogeneous medium.

Although there are, many articles available for solving the DPL model numerically and analytically, only very few finite element solutions are available for solving the DPL model due to the large discrepancy, identified by Al-Nimr and N. S. Al-Hunti (2000), exists between the analytical and finite element results. The reason for this discrepancy is due to the electron-phonon interaction term dominates and as a result, the overall temperature reached is higher than that predicted by the classical conduction equation. To overcome this in the finite element method, Siva Prakash *et al.* (2000) and Liu and Cheng (2006) used an analytical method to solve DPL when the value of $\tau_T > \tau_q$. Dhanaraj *et al.* (2019) used a three-time level finite difference scheme to resolve the dual-phase lag's heat conduction in a micro-scale gold film subjected to spontaneous temperature boundary conditions without knowing the heat flux. In the previous works, a complete finite element solution for the DPL problem is not given and the comparative temperature distribution of diffusive model, CV model, and DPL model at the same instant from transient to steady-state are not presented.

In the present work, one-dimensional dual-phase-lag heat conduction across a thin layer subjected to a constant temperature and insulated boundary conditions are predicted by using a complete finite element solution without using an analytical method for DPL when the value of $\tau_T > \tau_q$. The DPL model is solved to predict the temperature distribution across the thin layer using Python 3.6.3 after considering the relaxation time to heat flux τ_q and to the temperature gradient τ_T. The three different modes of heat conduction, diffusion (Fourier model), thermal wave (CV model), and dual-phase lag (DPL model), across the thin layer, are compared for the same instants against the initial and boundary conditions. The developed finite element DPL model is validated with the analytical solution given by Tzou (1995), numerical solutions given by Dhanaraj *et al.* (2019), and experimental work presented by Tang *et al.* (2007) with good agreement. Recently, Yuvaraj and Senthilkumar (2020) presented the length and time scale at which the thermal wave propagation vanishes from the CV model to the Fourier model. Also, to distinguish the diffusion, thermal wave, and DPL model, temperature variation at the center of the layer is predicted and shown that the speed of the thermal wave, infinite in the Fourier diffusion model and finite in both single and dual-phase lag are examined under transient to steady-state. Further, temperature contours plotted are evident for the DPL mode of heat conduction in a thin layer is entirely different from diffusion mode and thermal wave mode of heat conduction across the thin layer.

PROBLEM DESCRIPTION

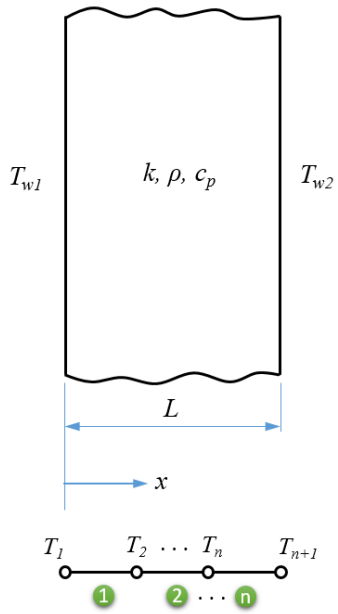

Figure 1. Thin layer subjected to symmetrical boundary conditions.

A thin layer of length L with thermal conductivity k, density ρ, and specific heat capacity c_p shown in Fig. 1 is subjected to two cases symmetrical and insulated boundary conditions respectively. In the first case, the left side and right side of the boundary are subjected to a constant temperature of $T_{w1} = T_{w2}$ maintained to be constant and in the second case, the left side boundary is maintained at a constant temperature T_{w1} and the right side boundary is insulated. When the heat is transferred from $x = 0$ to $x = L$, L is in macro size, the infinite speed of the thermal wave is assumed and followed by Fourier's mode of heat conduction across the thin layer. When L is in micro/nano-size, the finite speed of thermal waves caused the wave-like mode and DPL mode of heat conduction across the thin layer. In diffusion mode, the heat transfer is decided by thermal diffusivity α and in thermal wave mode of heat conduction, it is decided by thermal diffusivity and relaxation time τ. Whereas in the DPL mode of heat conduction, the heat transfer decided by thermal diffusivity, relaxation time for heat flux τ_q and relaxation time for temperature gradient τ_T. Heat transfer through a thin layer is assumed as one-dimensional and thermophysical properties are constant.

Governing equations

One dimensional heat conduction in a thin layer is governed by the Tzou (1995) DPL heat conduction equation and local energy balance equation.

The energy equation for anisotropic material can be written as

$$\nabla q = -\rho c_p \frac{\partial T}{\partial t} \tag{4}$$

where ρ is the density and c_p is the specific heat capacity. The given governing equations are in the form of dimensional characters are converted into non-dimensional form by using the following dimensionless parameters,

$$\xi = \frac{x}{L}, \eta = \frac{t\alpha}{l^2}, \theta = \frac{T_w - T}{T_w - T_0}, z_q = \frac{\tau_q \alpha}{l^2}, \quad z_T = \frac{\tau_T \alpha}{l^2}, \zeta = \frac{q}{q_r} \tag{5}$$

where ξ is the dimensionless distance in x direction as shown in Fig. 1, η is the dimensionless time, θ is the dimensionless temperature, z_q is the dimensionless heat flux relaxation time, z_T is the dimensionless temperature gradient relaxation time and ζ is the dimensionless heat flux. Rearranging Eqn. (1-4), the general form of DPL heatwave equation can be written as,

$$\alpha\, \tau_T \frac{\partial^3 T}{\partial x^2 \partial t} + \alpha \frac{\partial^2 T}{\partial x^2} = \tau_q \frac{\partial^2 T}{\partial t^2} + \frac{\partial T}{\partial t} \tag{6}$$

where α is thermal diffusivity ($\alpha = k/\rho c_p$). If $\tau_q = \tau_T = 0$, Eqn. (6) reduces to the first-order diffusion equation, $\tau_T = 0$ then Eqn. (6) becomes second-order thermal wave heat equation.

After substituting the non-dimensional terms from Eqn. (5) in to the Eqn. (6), the governing partial differential equation for one-dimensional DPL heat conduction equation can be given in the form of the dimensionless equation as

$$z_T \frac{\partial^3 \theta}{\partial \xi^2 \partial \eta} + \frac{\partial^2 \theta}{\partial \xi^2} = \mathrm{z_q} \frac{\partial^2 \theta}{\partial \eta^2} + \frac{\partial \theta}{\partial \eta} \tag{7}$$

Initial conditions:

$$\theta(\xi, \eta) = 1 \quad at \ \eta = 0, \qquad 0 < \xi < 1 \tag{8}$$

Boundary conditions:

Case – 1: The prescribed temperature at both side of the thin layer

$$\frac{\partial \theta}{\partial \eta}(\xi, \eta) = 0 \quad at \ \eta > 0, \xi = 0, \xi = 1 \tag{9}$$

$$\theta(\xi, \eta) = 1 \quad at \ \xi = 0, \quad \eta > 0 \tag{10}$$

$$\theta(\xi, \eta) = 1 \quad at \ \xi = 1, \quad \eta > 0 \tag{11}$$

Case – 2: The prescribed temperature at the left side and insulated at the right side of the thin layer

$$\theta(\xi, \eta) = 1 \quad at \ \xi = 0, \quad \eta > 0 \tag{12}$$

$$\zeta(\xi, \eta) = 0 \quad at \ \xi = 1, \quad \eta > 0 \tag{13}$$

The nodal temperatures T_2 to T_n as shown in Fig. 1 can be predicted by applying the initial and boundary conditions given in Eqn. (8-13) using the finite element method. The dimensionless temperature of 1 is maintained at the left and right side of the thin layer and maintained constant for case-1 and insulated condition for case-2. Initially, the temperature of the thin layer in length L is maintained at a dimensionless temperature of $\theta = 0$ at the dimensionless time is $\eta = 0$ and suddenly changed to the boundary conditions. The nodal temperatures are predicted by executing the finite element model using Python 3.6.3 (2020). The n numbers of linear algebraic equations are solved and the nodal temperatures and temperature contours are predicted by using the *NumPy* and *matplotlib* modules available in Python.

FINITE ELEMENT MODEL

In the finite element method, the given domain is discretized into several subdomains, called a finite element, the approximation functions of weighted-residual are constructed on each element for the solution of the problem. The step by step procedure followed in the present work to develop a finite element model is given by Reddy (2015).

The finite element model for the heat transfer problem, the one-dimensional steady-state without heat generation, can be developed by making a weak form of Eqn. (6)

$$z_T \frac{\partial^3 \theta}{\partial \xi^2 \partial \eta} + \frac{\partial^2 \theta}{\partial \xi^2} - \mathrm{z_q} \frac{\partial^2 \theta}{\partial \eta^2} - \frac{\partial \theta}{\partial \eta} = 0 \tag{14}$$

The finite element formulation for the governing equation (14) is,

$$\mathrm{z_q[M]}\{\ddot{\theta}\} + (\mathrm{[C] + z_T[K]})\{\dot{\theta}\} + \mathrm{[K]}\{\theta\} = \{\mathrm{F}\} \tag{15}$$

where, $[K] = \frac{1}{l}\begin{bmatrix} 1 & -1 \\ -1 & 1 \end{bmatrix}$ is the stiffness matrix, $[C] = \frac{l}{6}\begin{bmatrix} 2 & 1 \\ 1 & 2 \end{bmatrix}$ is the capacitance matrix, $[M]$ is the mass matrix, and $\{F\}$ is the force vector for a linear element. Eqn. (15) is the DPL mode of finite element model which contains a first-order time derivative $\{\dot{\theta}\}$ and second-

order time derivative $\{\ddot{\theta}\}$. The solution for the DPL heat equation in the form of a finite element model can be obtained using Newmark's scheme as follows

$$\dot{\theta}_{n+1} = \dot{\theta}_n + \Delta\eta((1-\gamma)\ddot{\theta}_n + \gamma\ddot{\theta}_{n+1} \tag{16}$$

$$\theta_{n+1} = \theta_n + \Delta\eta\theta_n + \Delta\eta^2\left(\frac{1}{2} - \beta\right)\ddot{\theta}_n \tag{17}$$

$$\mathrm{z_q[M]}\{\ddot{\theta}_{n+1}\} + ([\mathrm{C}] + \mathrm{z_T[K]})\{\dot{\theta}_{n+1}\} + [\mathrm{K}]\{\theta_{n+1}\} = \{\mathrm{F}_{n+1}\} \tag{18}$$

The value of γ and β are taken as $\frac{1}{2}$ and $\frac{1}{4}$ respectively. By applying initial and boundary conditions as given in Eqn. (8-13), first the value of $\ddot{\theta}_n$ can be obtained by solving Eqn. (15). The finite-difference form of $\ddot{\theta}_n$ can be written as

$$\{\ddot{\theta}_n\} = \frac{\dot{\theta}_{n+1} - \dot{\theta}_n}{\Delta\eta} \tag{19}$$

After finding $\ddot{\theta}_n$, substitute it in Eqn. (19) to find $\dot{\theta}_{n+1}$ and from Eqn. (16) the value of $\ddot{\theta}_{n+1}$ can be obtained. The value of θ_{n+1} for the first time step can be obtained from Eqn. (17) and repeating this procedure for the consecutive time steps. Then Eqn. (18) is the element level DPL heat equation for $n+1^{th}$ time step.

RESULTS AND DISCUSSION

Mesh sensitivity test

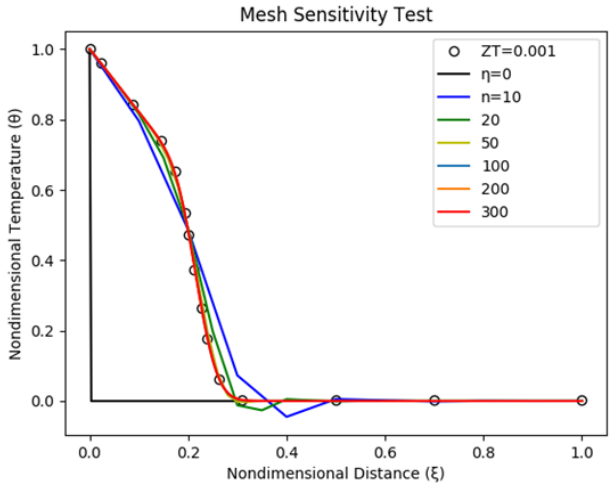

Figure 2. Mesh sensitivity test.

The mesh sensitivity study was conducted for the range of several elements from 10 to 300. Fig. 2 shows the propagation of the thermal wave, at $Z_q = 0.05$, $Z_T = 0.001$ and $\eta = 0.045$, for a different number of elements. The non-dimensional temperature variation is negligible for the mesh 200 and 300 elements. When the time scale increases the convergent solution for the present model requires more number of elements than 200. Hence, 300 elements and time step 10^{-4} have been chosen for the execution of all the three models from transient to steady-state. The temperatures of each nodal point are predicted by solving Eqn. (15-19) for DPL heat transfer across a thin layer. The code is generated and the finite element model is solved by using Python 3.6.3 (2020), an open-source software.

Validation of the present model with the Analytical and Numerical solutions

The present finite element model is validated with the analytical solution given by Tzou (1995) for different Z_T values as shown in Fig. 3 (a). Tzou considered the dimensionless heat flux relaxation time $Z_q = 0.05$ and varied the dimensionless temperature gradient relaxation time Z_T and found that when $Z_T > 0.05$ the heat conduction follows the dual-phase lag model. All three models, $Z_T = 0.001$, $Z_T = 0.05$ and $Z_T = 0.5$ validated with the analytical solution with good agreement. The present model is also compared and validated with the numerical solution given by Dhanaraj *et al.* (2019) for different dimensionless times $\eta = 0.02$, $\eta = 0.05$, and $\eta = 0.16$. The similar kind of boundary conditions used and obtained good results as shown in Fig. 3 (b).

Fig. 3 (c) shows the validation of present model with experimental work presented by Tang *et al.* (2007). They conducted an experiment for DPL heat conduction in meat specimens with three different thickness 2 mm, 3 mm and 4 mm by using 1 sec IR light pulse. The experimental result for 2 mm specimen is used to validate with the present work shows very good agreement than the Fourier and CV model. The table of errors for different mode of heat transfer Fourier model, CV model and DPL model of analytical data are compared with the present numerical data and obtained the positive errors of 2.2% for Fourier model, 0.67% for CV model, and negative errors 0.41% for DPL model.

Case-1: Comparison of diffusion model, CV model, and DPL model

In case-1, the temperature of $\theta = 1$ is maintained constantly on both side of the thin layer and the heat flux relaxation time Z_q is taken as 0.05 and the temperature gradient relaxation time Z_T is varied from $0 - 0.5$ similar to the work carried numerically by Dhanaraj *et al.* (2019). Then Eqn. (14) can be reduced to the diffusion model when $Z_q = Z_T = 0$ and CV model when $Z_T = 0$. The dual-phase lag model predicts the précised temperature variation across the thin layer when $Z_T > 0$. In the present work, the value of $Z_T = 0$ is considered as CV model, the value of $Z_T = 0.05$ is taken as the diffusion model and other non zero values of Z_T are taken as the DPL model.

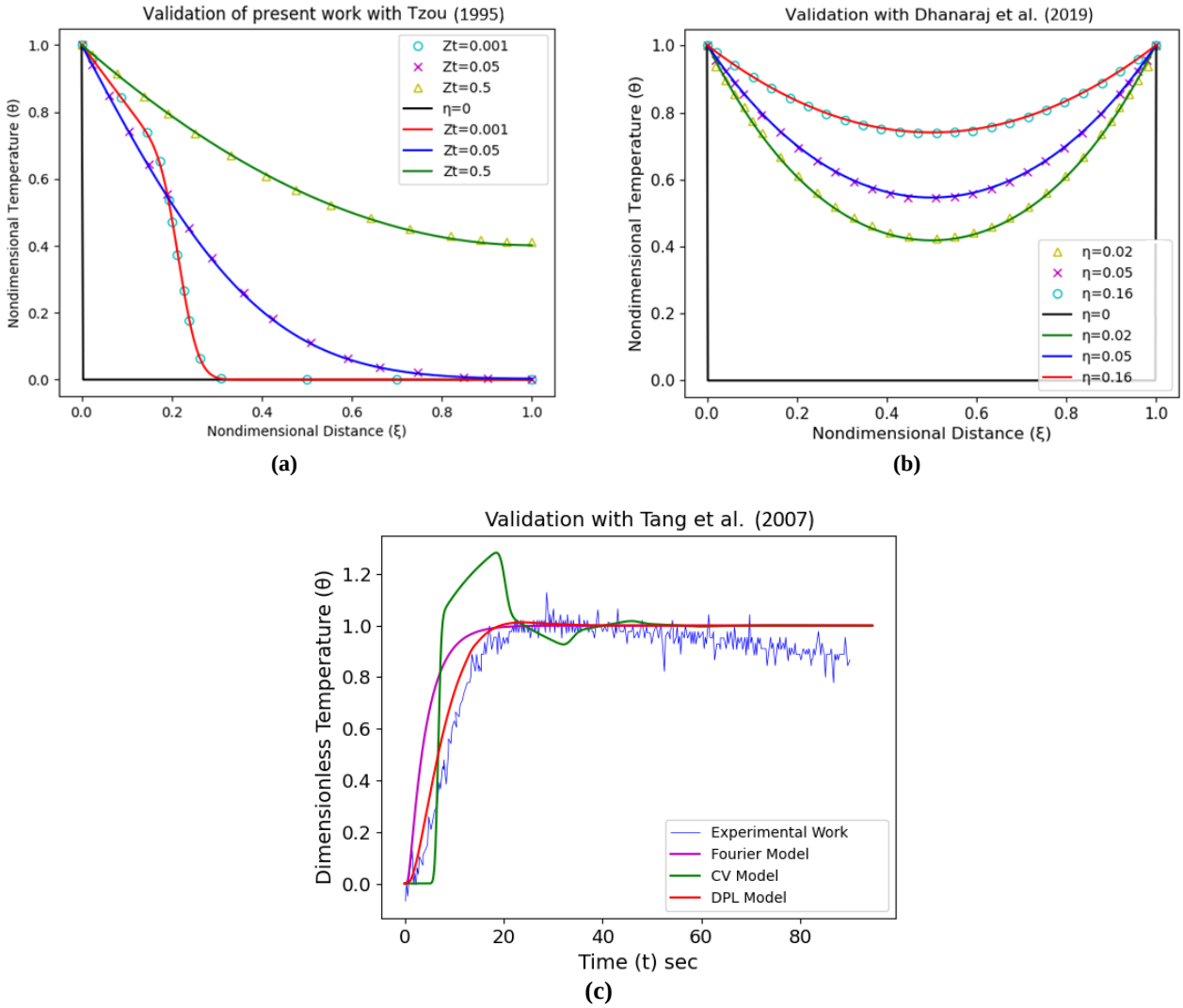

Figure 3. Validation of present model with (a) Analytical solution given by Tzou (1995), (b) Numerical solution presented by Dhanaraj et al. (2019) and (c) Experimental work presented by Tang et al. (2007).

Table 1. Present numerical work error table.

Fourier model			**CV model**			**DPL model**		
Analytical work	**Present work**	**Error %**	**Analytical work**	**Present work**	**Error %**	**Analytical work**	**Present work**	**Error %**
1.0000	1.0000	**0.0000**	1.0000	1.0000	**0.0000**	0.9976	0.9976	**0.0000**
0.9398	0.9373	**0.2564**	0.9639	0.9542	**1.0000**	0.9735	0.9735	**0.0000**
0.8482	0.8458	**0.2841**	0.8410	0.8434	**-0.2865**	0.9084	0.9108	**-0.2653**
0.7398	0.7373	**0.3257**	0.7373	0.7373	**0.0000**	0.8410	0.8458	**-0.5731**
0.6434	0.6337	**1.4981**	0.6530	0.6458	**1.1070**	0.7880	0.7928	**-0.6116**
0.5518	0.5494	**0.4367**	0.5349	0.5325	**0.4505**	0.7301	0.7349	**-0.6601**
0.4506	0.4482	**0.5348**	0.4699	0.4675	**0.5128**	0.6651	0.6699	**-0.7246**
0.3639	0.3590	**1.3245**	0.3711	0.3663	**1.2987**	0.6024	0.6120	**-1.6000**
0.2578	0.2530	**1.8692**	0.2651	0.2602	**1.8182**	0.5614	0.5663	**-0.8584**
0.1807	0.1759	**2.6667**	0.1735	0.1663	**4.1667**	0.5157	0.5229	**-1.4019**
0.1108	0.1060	**4.3478**	0.0602	0.0602	**0.0000**	0.4747	0.4795	**-1.0152**
0.0627	0.0602	**3.8462**	0.0024	0.0024	**0.0000**	0.4434	0.4458	**-0.5435**
0.0361	0.0361	**0.0000**	0.0000	0.0000	**0.0000**	0.4265	0.4217	**1.1299**
0.0217	0.0200	**7.8833**	0.0000	0.0000	**0.0000**	0.4120	0.4120	**0.0000**
0.0048	0.0042	**12.2500**	0.0000	0.0000	**0.0000**	0.4024	0.4024	**0.0000**
Average Fourier model error		**2.2 %**	Average CV model error		**0.67 %**	Average DPL model error		**0.41 %**

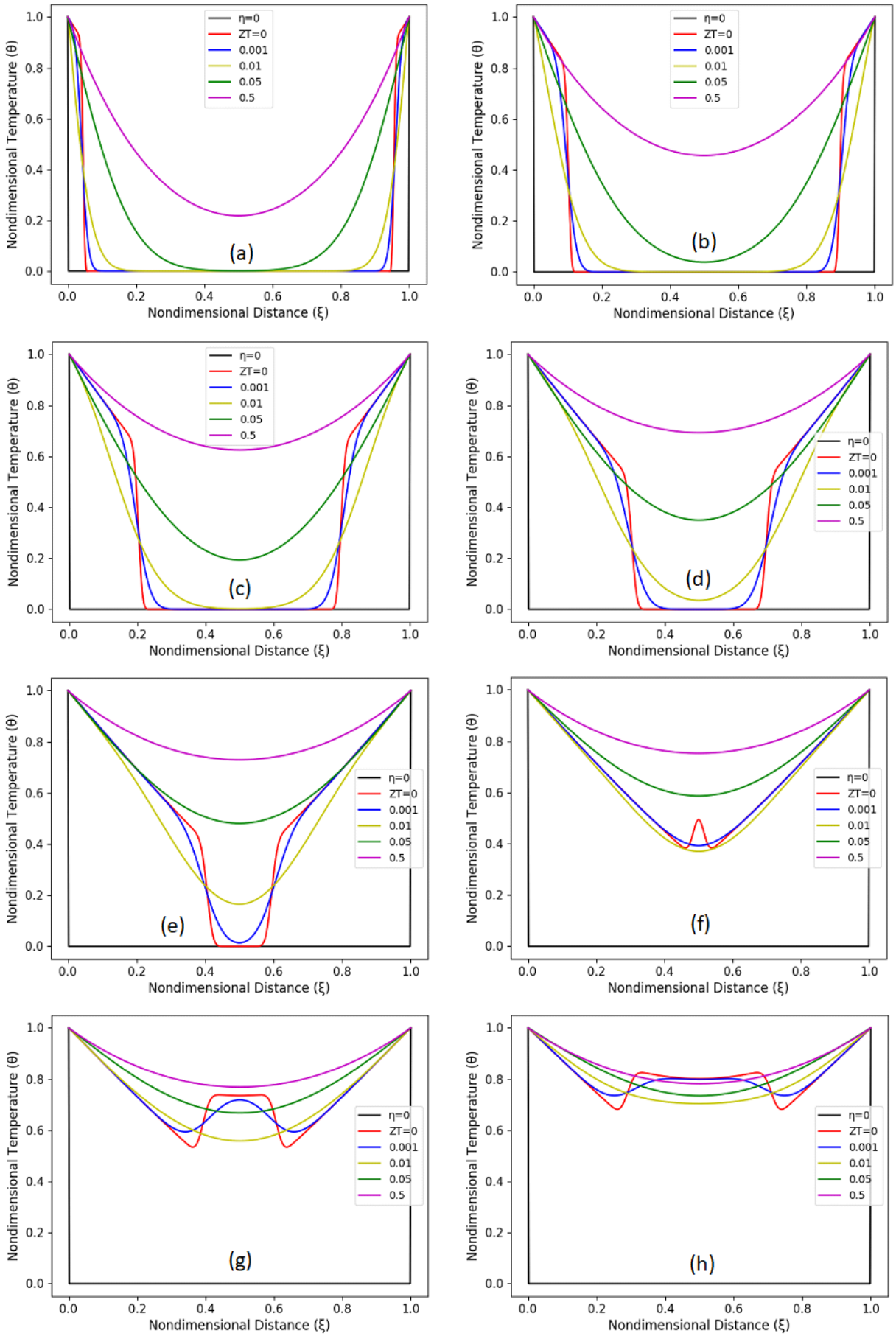

Figure 4. Case-1 Temperature variation for different Z_T, (a) $\eta = 0.01$, (b) $\eta = 0.02$, (c) $\eta = 0.045$, (d) $\eta = 0.068$, (e) $\eta = 0.091$, (f) $\eta = 0.114$, (g) $\eta = 0.136$, and (h) $\eta = 0.159$.

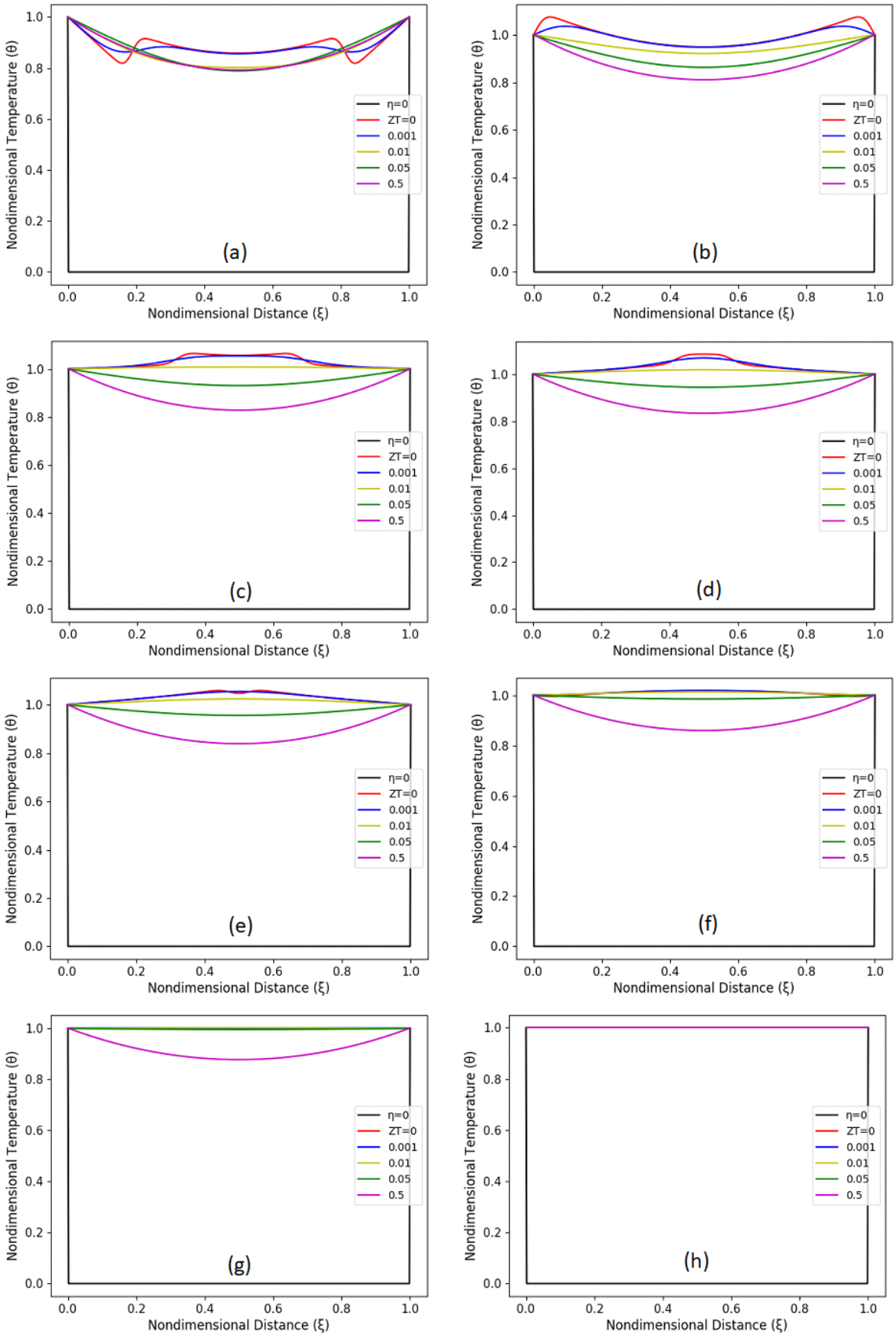

Figure 5. Case-1 Temperature variation for different Z_T, (a) $\eta = 0.182$, (b) $\eta = 0.227$, (c) $\eta = 0.295$, (d) $\eta = 0.318$, (e) $\eta = 0.341$, (f) $\eta = 0.432$, (g) $\eta = 0.568$, and (h) $\eta = 2.468$.

Case-1: Temperature contours

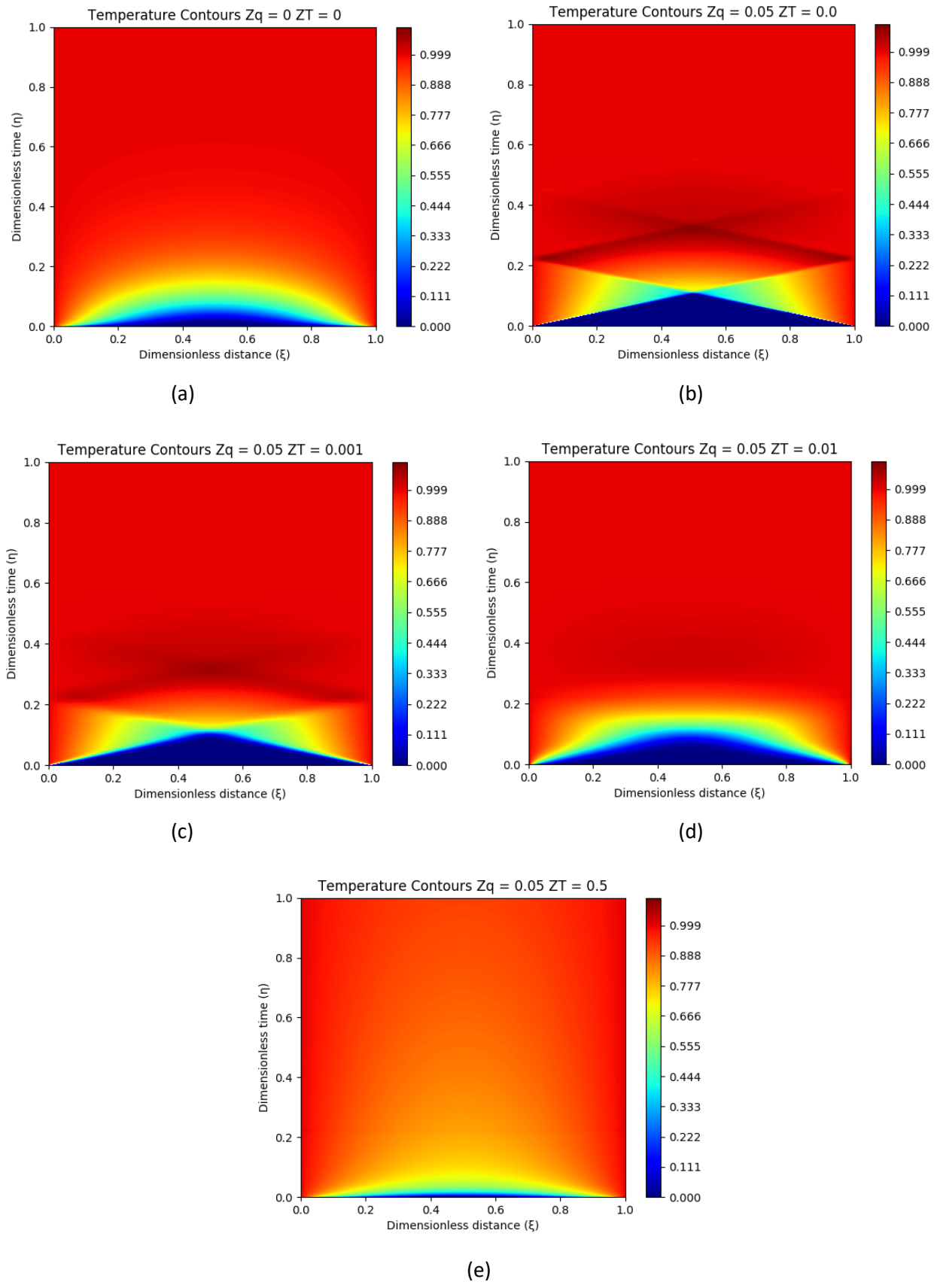

Figure 6. Case-1 Temperature contours, (a) Diffusion model $Z_q = Z_T = 0$, (b) CV model $Z_T = 0$, (c) DPL model $Z_T = 0.001$, (d) DPL model $Z_T = 0.01$, (e) DPL model $Z_T = 0.5$.

The variation of temperature for different Z_T values from $0-0.5$ are shown in Fig. 4 (a-h) and Fig. 5(a-h) for different time η. Fig. 4(a) shows the temperature variation across the thin layer, at $\eta = 0.01$, due to heat conduction. Thermal wave-like temperature variation occurs, when $Z_T = 0$, due to only the heat flux relaxation time Z_q exist in a thin layer. The diffusion mode of heat conduction occurs at $Z_q = Z_T = 0.05$ and the thermal wave propagates smoothly without any collision as shown in Fig. 4(b-e). The thermal wave speed is assumed as infinite in the diffusion mode of heat conduction and finite in the CV model and DPL model. Fig. 4 (f) shows the collision of thermal wave occurs at the center of the layer at $\eta = 0.114$ and the temperature increases after the collision and propagates in reverse order towards either side of the boundary. The dual lag affects the propagation time and both diffusion and CV model catching the DPL model at $\eta = 0.182$ and overtake afterward which is clearly shown in Fig. 5 (a). From Fig. 5 (b-e) it is noted that the DPL model propagates slower than the diffusion and CV model to reach a steady state. The diffusion model reaches a steady-state first at time $\eta = 0.432$, Fig. 5 (f), second CV model at $\eta = 0.568$, Fig. 5 (g), finally DPL model at $\eta = 2.468$ as shown in Fig. 5 (h).

The temperature contours are plotted for different conditions, the diffusion model $Z_q = Z_T = 0$, the CV model $Z_T = 0$, DPL model $Z_T = 0.001$, DPL model $Z_T = 0.01$ and DPL model $Z_T = 0.5$ as shown in Fig. 6 (a-e) respectively. In the diffusion model, there is no lag, $Z_q = Z_T = 0$, in response between applied heat flux and the temperature gradient, causes no collision in the thin layer. The immediate response of temperature gradient against the applied heat flux causes smooth conduction of heat across the thin layer and the temperature contours from $\eta = 0$ to $\eta = 1$ is shown in Fig. 6 (a). Whereas in Fig. 6 (b), the evidence of collision is clearly shown as the triangular contours with sharp corners. The thermal wave propagates with relaxation time $Z_q = 0.5$ and $Z_T = 0$. Each sharp corner represents the occurrence of collisions and five times the collision consecutively happens at the center of the layer and boundary of the layer. The first collision of thermal wave occurred at $\xi = 0.5$ and $\eta = 0.114$ with an increase in temperature and move towards either side of the boundary. The second collision occurs at the boundary of the layer and propagates back towards the center of the layer with a further increase in temperature. After the third collision at the center of the layer the temperature decreases and repeats alternatively and after fifth collision smooth propagation occurred. In DPL model, Fig. 6 (c-e), both relaxation time Z_T and Z_q are considered and the wave-like heat propagation disappears and propagates slower than the diffusion and CV model. In Fig. 6 (c), the sharp corners have vanished and the triangular shape of contours are smudged due to relaxation time $Z_T = 0.001$. Fig. 6 (d) shows that the increase in relaxation time $Z_T = 0.01$ the wave-like propagation are disappeared and transition from CV mode of heat conduction to DPL mode of heat conduction happened. The temperature contours for $Z_T = 0.5$ is shown in Fig. 6 (e) is the complete evidence for the DPL mode of heat conduction in entirely different from diffusion and CV mode of heat conduction.

Case-1: Temperature variation at the center of the layer $\xi = 0.5$

The heat conduction model number, $F_T = \frac{\tau_T}{\tau_q}$ [26], is used to analyze the temperature variation at the center of the layer $\xi = 0.5$. The Fig. 7 (a-d) shows the temperature variation at the center of the layer for different values of F_T from time $\eta = 0$ to $\eta = 1$. When $\tau_T = 0$, heat conduction model number F_T becomes zero and the heat propagates like a wave across the thin layer followed by the CV model with single relaxation time. When $F_T = 1$, both relaxation times are equal in magnitude and it follows the diffusion mode of heat conduction. When $F_T < 1$, it follows the DPL mode of heat conduction followed by the transition from the CV model to the diffusion model. Whereas $F_T > 1$, diffusion mode is changed to the DPL mode of heat conduction.

Fig. 7 (a) shows that the temperature variation at the center of the layer $\xi = 0.5$ from $\eta = 0$ to $\eta = 0.1$. The temperature remains in the initial state, $\theta = 0$, for CV model up to $\eta = 0.1$ and $F_T = 0$. Whereas $F_T > 0$, in case of diffusion and DPL model, the temperature at the center of the layer varies earlier than the CV model. At $\eta = 0.114$ and $F_T = 0$, the thermal wave from either side of the boundary reaches the center of the layer and causes the first collision to occur at $\xi = 0.5$. After the first collision, the temperature increases immensely from $\theta = 0$ to $\theta = 0.7$ as shown in Fig. 7 (b) and then it continuously increases the temperature and reaches maximum temperature $\theta = 1.1$ which is greater than the applied boundary condition. This unrealistic phenomenon is the main cause for considering the DPL mode of heat conduction across the thin layer. At time $\eta = 0.2$, the temperature at the center of the layer is greater for the CV model $F_T = 0$ and smaller for diffusion and DPL model $F_T > 0$. After time $\eta = 0.3$, the collision of the thermal wave, $F_T = 0$ decreases the temperature at the center of the layer as shown in Fig. 7 (c) and it follows the diffusion model, $F_T = 1$. After time $\eta = 0.6$ onwards, CV model and DPL model $F_T = 0.25$ follows a similar way of diffusion model as clearly shown in Fig. 7 (d). The temperature at the center in the DPL model, when $F_T > 1$, are smaller than the diffusion and CV model at time $\eta = 1$.

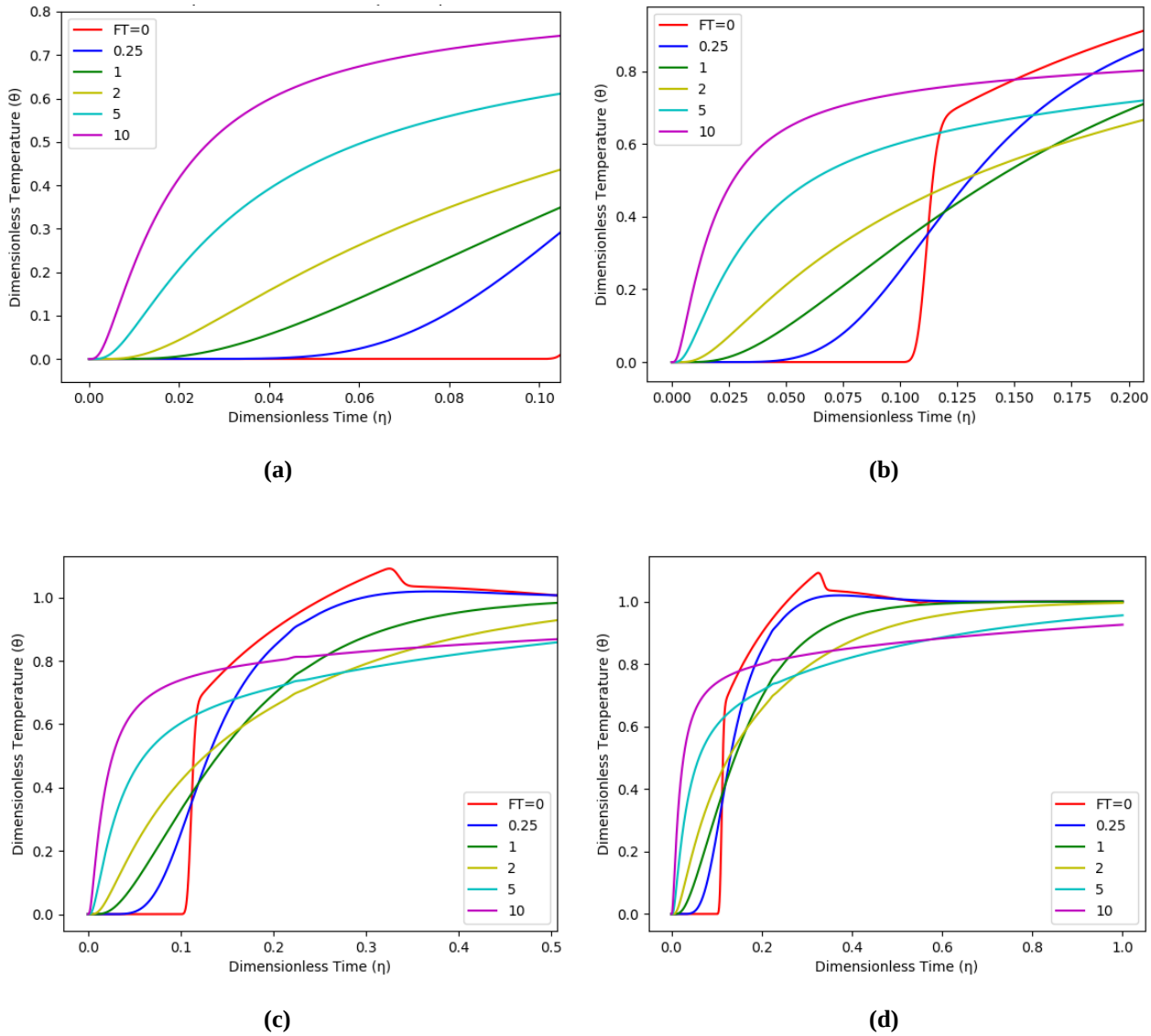

Figure 7. Case-1 Temperature variation at $\xi = 0.5$ for different F_T, (a) up to $\eta = 0.1$, (b) up to $\eta = 0.2$, (c) up to $\eta = 0.5$ and (d) up to $\eta = 1$

Case-2: Comparison of diffusion model, CV model and DPL model

In case-2, the temperature of $\theta = 1$ is maintained constant at left side boundary of the thin layer and insulated boundary condition is taken at right side of the boundary. The relaxation times Z_q and Z_T are varied similar to that of case-1. The initial and boundary conditions given in Eqn. (8-11) and the Eqn. (14-19) are applied to solve the DPL model for insulated boundary condition and the temperature variations from transient state to steady state are shown in Fig. 8 (a-h) and Fig. 9 (a-h).

Fig. 8 (a) shows the temperature variation at $\eta = 0.023$ in which the DPL model with $Z_T = 0.5$ reaches the right boundary earlier than the diffusion and CV model. The diffusion model with $Z_T = 0.5$ marching towards the right insulated boundary faster than the DPL model, with $Z_T = 0.01$ and $Z_T = 0.001$, and CV model with $Z_T = 0$ as shown in Fig. 8 (b). At time $\eta = 0.068$, Fig. 8 (c) shows the diffusion model reaches the right side boundary and still the DPL model, with $Z_T = 0.01$ and $Z_T = 0.001$, and the CV model are well behind the diffusion model. After time $\eta = 0.114$, there is no collision occurs at the center of the layer $\xi = 0.5$ due to there is no source of heat comes from the right side boundary and the thermal wave propagates towards the right side boundary as shown in Fig. 8 (d-e). The CV model finally reaches the right side boundary after time $\eta = 0.205$, Fig. 8 (f-h), and makes the first collision at the right side of the boundary with an increase in temperature. After the first collision, reverse propagation occurs towards the left side boundary of the thin layer as shown in Fig. 9 (a-b). The diffusion model, CV model and DPL model with $Z_T = 0.001$, $Z_T = 0.01$ are chasing

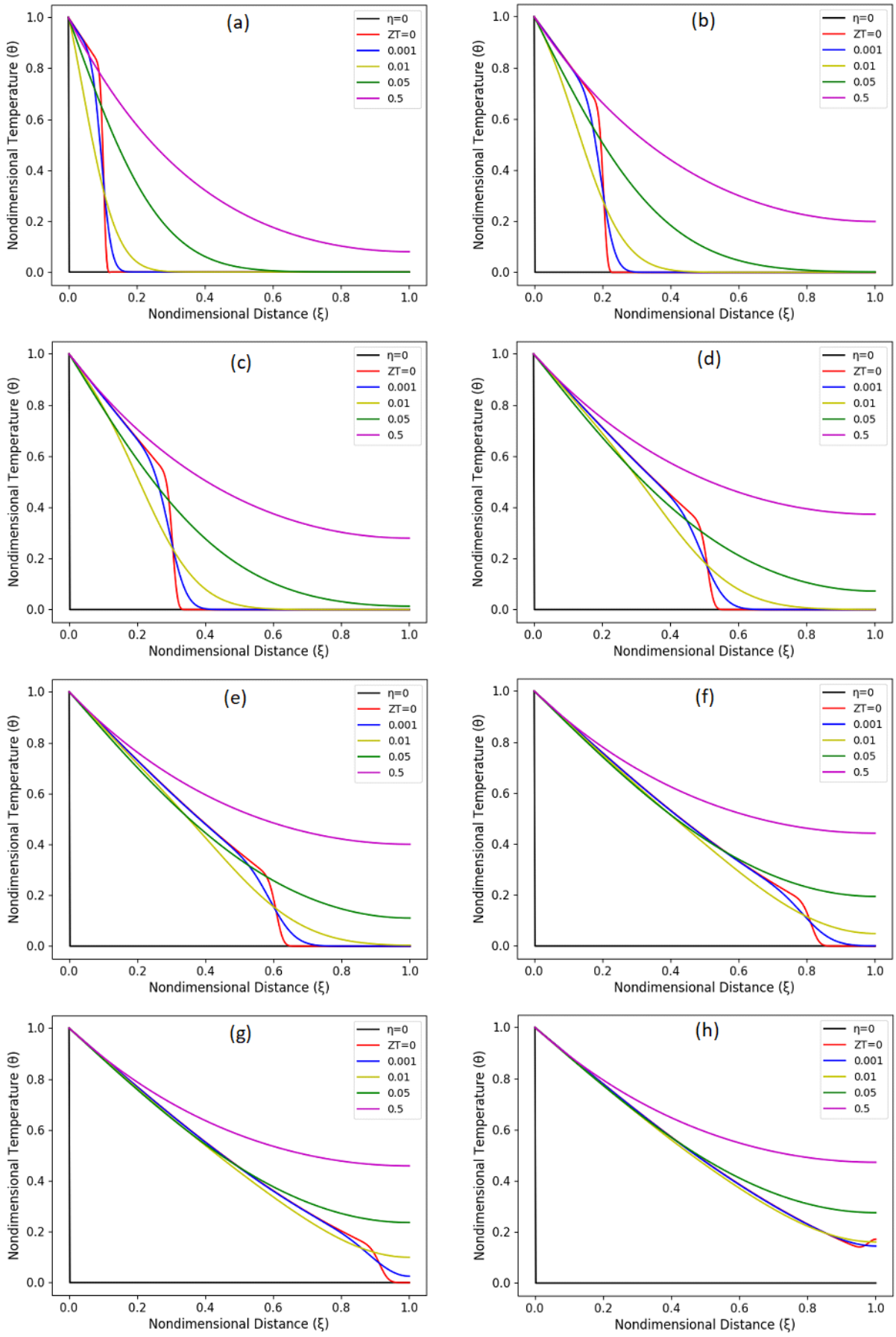

Figure 8. Case-2 Temperature variation for different Z_T, (a) $\eta = 0.023$, (b) $\eta = 0.045$, (c) $\eta = 0.068$, (d) $\eta = 0.114$, (e) $\eta = 0.136$, (f) $\eta = 0.182$, (g) $\eta = 0.205$, and (h) $\eta = 0.227$.

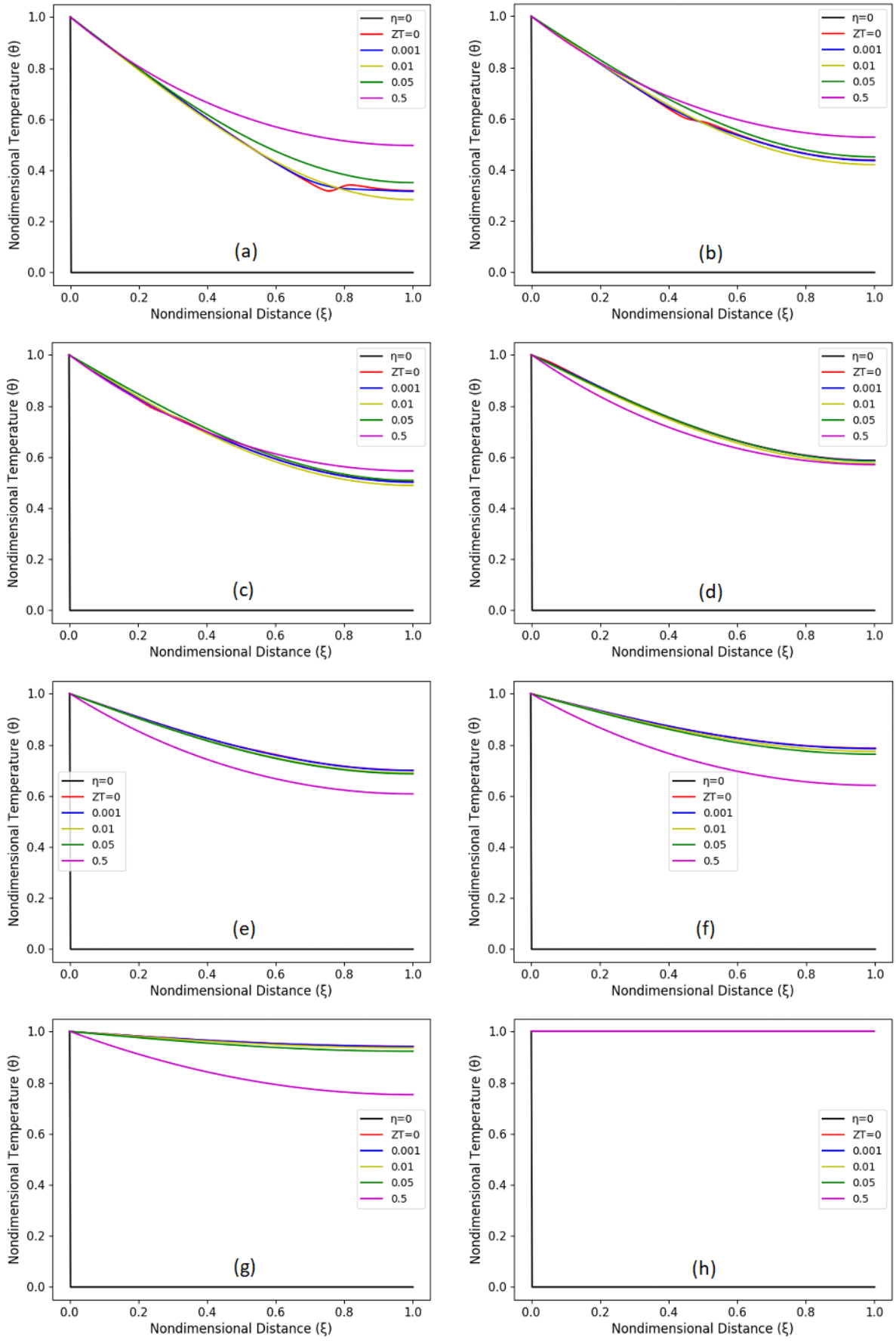

Figure 9. Case-2 Temperature variation for different Z_T, (a) $\eta = 0.273$, (b) $\eta = 0.341$, (c) $\eta = 0.386$, (d) $\eta = 0.454$, (e) $\eta = 0.568$, (f) $\eta = 0.682$, (g) $\eta = 1.136$, and (h) $\eta = 4.122$.

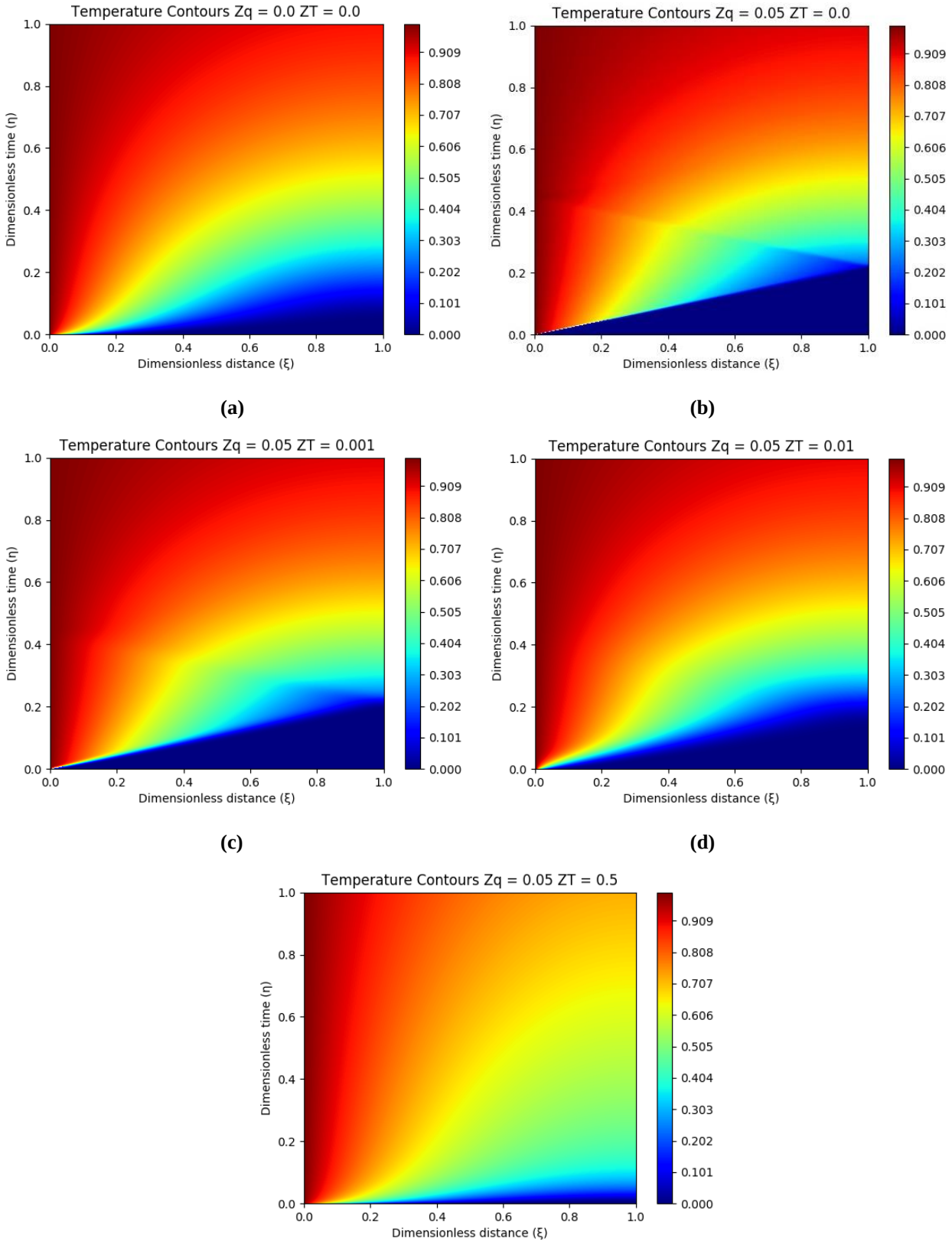

(a) **(b)** **(c)** **(d)** **(e)**

Figure 10. Case-2 Temperature contours, (a) Diffusion model $Z_q = Z_T = 0$, (b) CV model $Z_T = 0$, (c) DPL model $Z_T = 0.001$, (d) DPL model $Z_T = 0.01$, (e) DPL model $Z_T = 0.5$.

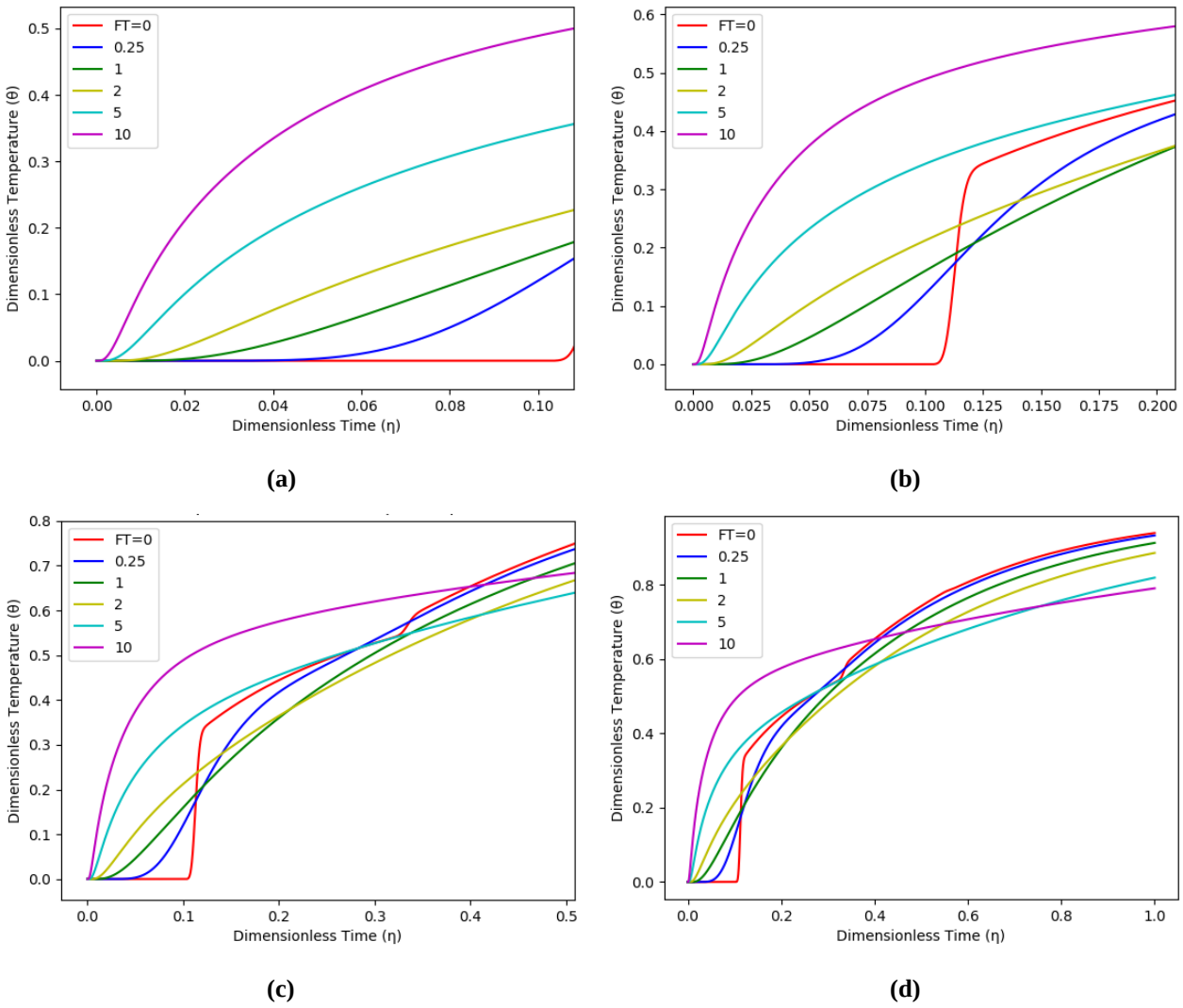

Figure 11. Case-2 Temperature variation at $\xi = 0.5$ for different F_T, (a) up to $\eta = 0.1$, (b) up to $\eta = 0.2$, (c) up to $\eta = 0.5$ and (d) up to $\eta = 1$.

the DPL model with $Z_T = 0.5$, Fig. 9 (c) and overtakes at $\eta = 0.454$ as shown in Fig. 9 (d). This lag in heat propagation across the thin layer is caused by the large value of relaxation time $Z_T = 0.5$ and the other model marching towards steady state are shown in Fig. 9 (e-g). The CV model first reaches a steady state at time $\eta = 1.212$ then the diffusion model reaches a steady state at tine $\eta = 1.286$ and finally DPL model with $Z_T = 0.5$ reaches a steady state at $\eta = 4.122$ as shown in Fig. 9 (h).

Case-2: Temperature contours

The temperature contours are plotted for different conditions, diffusion model $Z_q = Z_T = 0$, CV model $Z_T = 0$, DPL model $Z_T = 0.001$, DPL model $Z_T = 0.01$ and DPL model $Z_T = 0.5$ as shown in Fig. 10 (a-e) respectively. In diffusion model there is no lag in heat flux. $Z_q = 0$, and temperature gradient, $Z_T = 0$. The response between applied heat flux to the temperature gradient is instantly obtained and no collision occurs anywhere across the thin layer. The immediate response of temperature gradient against the applied heat flux causes smooth conduction of heat across the thin layer for the diffusion model and the temperature contours from $\eta = 0$ to $\eta = 1$ is shown in Fig. 10 (a). Whereas in Fig. 10 (b), the evidence of collision is clearly shown as the triangular contours with sharp corners for the CV model with relaxation time $Z_q = 0.5$ and $Z_T = 0$. The first collision of the thermal wave occurs at the right side boundary at $\xi = 1$ and $\eta = 0.214$ then it follows reverse propagation and reaches the left side boundary at $\eta = 0.454$ with the second collision. After the second collision the temperature decreases and the CV model marching towards a steady-state without any further collision. Fig. 10 (c) and Fig. 10 (d) are the shreds of evidence of vanishing sharp corners and the thin layer follows DPL mode of heat conduction with $Z_T = 0.001$ and $Z_T = 0.01$ respectively.

It is noted that, from Fig. 10 (a-e), the DPL mode of heat conduction is entirely different from the diffusion model and CV model. The maximum temperature zone is nearer to the left boundary at $\xi = 0$ in case of DPL model with

$Z_T = 0.5$ as shown in Fig. 10 (e). Whereas in the diffusion model, Fig. 10 (a), the maximum temperature zone uniformly distributed towards the right side of the boundary. This is due to the presence of both relaxation time Z_q and Z_T, decreases the response between given heat flux and temperature gradient. In the DPL model, the heat propagates slowly and reaches a steady-state after diffusion model and the CV model. For example, take gas turbine blade, the ceramic thin coating are used as thermal barriers with thermal diffusivity of $\alpha = 1.16 \times 10^{-7}$ m^2/s, coating thickness of $x = 1$ μm, initiall all the points the temperature is assumed as 303 K, one side of the blade is suddenly exposed to a temperature of 373 K. After time $t \approx 9$ μs, at the center of the thin layer $x = 0.5$ μm, the temperature becomes $T \approx 317$ K for DPL mode of heat transfer. Whereas, for the same condition the temperature becomes $T \approx 307$ K for CV model and $T \approx 310$ K for Fourier model. The Fourier model and CV model reaches steady state faster than the DPL model due to the dual relaxation time responses.

Case-2: Temperature variation at the center of the layer $\xi = 0.5$

The temperature variation at the center of the thin layer $\xi = 0.5$ for different values of F_T from time $\eta = 0$ to $\eta = 1$ are shown in Fig. 11 (a-d). From Fig. 11 (a) it is noted that, the CV model $F_T = 0$, the temperature remains in the initial state, $\theta = 0$, up to $\eta = 0.1$. Whereas in the case of diffusion and DPL model, $F_T > 0$, the temperature at the center of the layer varies earlier than the CV model similar to case-1. At $\eta = 0.114$ and $F_T = 0$, the thermal wave from the left side of the boundary meets the center of the layer and propagates without any collision at $\xi = 0.5$. The rise in temperature shown in Fig. 11 (b) for $F_T = 0$ is the immediate response of temperature gradient with the absence of τ_T. At $\eta = 0.2$, the temperature at the center of the layer for the CV model and DPL model are greater than the diffusion model. The second rise in temperature, at $\eta = 0.342$ as shown in Fig. 11 (c), for the CV model, is happened due to the first collision occurs in the right side boundary and reverse propagation of thermal wave towards the left side boundary. At $\eta = 0.5$, the temperature at the center of the layer reduces for $F_T > 1$ and increase for $F_T < 1$ compared to the diffusion model $F_T = 1$. When the time moves on and becomes $\eta = 1$, the temperature variation is shown in Fig.11 (d) and DPL model with $F_T = 10$ the temperature further decreases than the that of DPL model with $F_T = 5$. From Fig. 11 (d), it is noted that when the conduction number F_T increases the temperature decreases after time $\eta = 1$ and when F_T decreases the temperature increases after time $\eta = 1$.

CONCLUSION

The finite element model for dual phase-lag heat conduction across a thin layer is developed successfully to predict the temperature when it is subjected to two cases, case-1 constant temperature at both sides and case-2 left side constant temperature and right side insulated condition. The developed code is executed in Python 3.6 and the obtained results are validated with analytical, numerical, and experimental results with excellent agreement. Uniquely in this work, a comparative study of diffusion mode, CV mode, and DPL mode of heat conduction across the thin layer is examined numerically from transient to steady-state. The temperature contours are plotted for all three conditions and the way it propagates differently through the thin layer is clearly shown. Further, the temperature variation at the center of the layer, at which collision occurred, is predicted and the speed of the thermal wave, infinite in the Fourier diffusion model and finite in both single and dual-phase lag, is examined under transient to steady-state condition.

The temperature contours for different z_q and z_T are plotted and revealed the way of diffusion model with $z_q = z_T = 0$, the CV model with $z_T = 0$, and DPL model $z_q > 0$ and $z_T > 0$ follows a different way. Also, the temperature variation at the center of the layer is analyzed for both the cases. It is found that, the diffusion model with the conduction number $F_T = 1$ reaches steady state first at time $\eta = 0.432$, CV model and DPL model with $F_T < 1$ reaches steady sate second at time $\eta = 0.568$ and DPL mode with $F_T > 1$ reaches steady-state finally at $\eta = 2.468$.

REFERENCES

Al-Nimr M. A., Naser S. Al-Huniti, 2000, Transient Thermal Stresses In A Thin Elastic Plate Due To A Rapid Dual-Phase-Lag Heating, *Journal of Thermal Stresses*, 23, 8, 731-746.

Antaki P. J., 1998, Solution for non-Fourier dual phase lag heat conduction in a semiinfinite slab with surface heat flux, *International Journal of Heat and Mass Transfer*, 41, 14, 2253-2258.

Cattaneo C., 1958, Sur une forme de l'equation de la chaleur eliminant la paradoxe d'une propagation instantantee, *Compt. Rendu*, 247, 431-433.

Dhanaraj S. N., Karthikeya Sharma T., Amba Prasad Rao G., and Madhu Murthy K., 2019, Numerical Technique for Resolving the Dual Phase Lag Heat Conduction in Thin Film Metal, *Heat Transfer Engineering*, 41, 6-7, 665-675.

Elsayed-Ali H. E., Juhasz T., Smith G. O., and Bron W. E., 1991, Femtosecond thermoreflectivity and thermotransmissivity of polycrystalline and single-crystalline gold films, *Physical Review B*, 43, 5, 4488-4491.

Fong E. and Lam T. T., 2014, Asymmetrical collision of thermal waves in thin films: An analytical solution, *International Journal of Thermal Sciences*, 77, 55-65.

Fujimoto J. G., Liu J. M., Ippen, E. P. and Bloembergen, N., 1984, Femtosecond Laser Interaction with Metallic Tungsten and Nonequilibrium Electron and Lattice Temperatures, *Physical Review Letters*, 53, 19, 1837-1840.

Hector L. G., Kim W. S. and Özisik M. N., 1992, Hyperbolic heat conduction due to a mode locked laser pulse train, *International Journal of Engineering Science*, 30, 12, 1731-1744.

Körner C. and Bergmann H. W., 1998, The physical defects of the hyperbolic heat conduction equation, *Applied Physics A*, 67, 4, 397-401.

Lam T. T. and Fong E., 2011, Heat diffusion vs. wave propagation in solids subjected to exponentially-decaying heat source: Analytical solution, *International Journal of Thermal Sciences*, 50, 11, 2104-2116.

Lewandowska M. and Malinowski L., 2006, An analytical solution of the hyperbolic heat conduction equation for the case of a finite medium symmetrically heated on both sides, *International Communications in Heat and Mass Transfer*, 33, 1, 61-69.

Li J., Cheng P., Peterson G. P. and Xu J. Z., 2005, Rapid Transient Heat Conduction In Multilayer Materials With Pulsed Heating Boundary, *Numerical Heat Transfer, Part A: Applications*, 47, 7, 633-652.

Liu K. C., and Cheng P. J., 2006, Numerical Analysis for Dual-Phase-Lag Heat Conduction in Layered Films, *Numerical Heat Transfer, Part A: Applications*, 49, 6, 589-606.

Majumdar A., 1993, Microscale Heat Conduction in Dielectric Thin Films, *Journal of Heat Transfer*, 115, 1, 7-16.

Mitra K., Kumar S., Vedevarz A., and Moallemi M. K., 1995, Experimental Evidence of Hyperbolic Heat Conduction in Processed Meat, *Journal of Heat Transfer*, 117, 3, 568-573.

Python 3.6.3, https://www.python.org/

Qiu T. Q., and Tien C. L., 1992, Short-pulse laser heating on metals, *International Journal of Heat and Mass Transfer*, 35, 3, 719-726.

Reddy J. N., 2015, *An Introduction to the Finite Element Method*, McGraw Hill Education (India) Private Limited, New Delhi.

Siva Prakash G., Sreekanth Reddy S., Sarit K. Das, Sundararajan T., and Seetharamu K. N., 2000, Numerical Modelling Of Microscale Effects In Conduction For Different Thermal Boundary Conditions, *Numerical Heat Transfer, Part A: Applications*, 38, 5, 513-532.

Tan Z. M., and Yang W. J., 1997, Heat transfer during asymmetrical collision of thermal waves in a thin film, *International Journal of Heat and Mass Transfer*, 40, 17, 3999-4006.

Tan Z. M., and Yang, W. J., 1997, Non-Fourier Heat Conduction in a Thin Film Subjected to a Sudden Temperature Change on Two Sides, *Journal of Non-Equilibrium Thermodynamics*, 22, 1, 75.

Tang D., Araki N., and Yamagishi N., 2007, Transient temperature responses in biological materials under pulsed IR irradiation, *Heat and Mass Transfer*, 43, 6, 579-585.

Tang D. W., and Araki N., 2000, Non-fourier heat condution behavior in finite mediums under pulse surface heating, *Materials Science and Engineering: A*, 292, 2, 173-178.

Torii S., and Yang W. J., 2005, Heat transfer mechanisms in thin film with laser heat source, *International Journal of Heat and Mass Transfer*, 48, 3, 537-544.

Tzou D. Y., 1995, Experimental support for the lagging behavior in heat propagation, *Journal of Thermophysics and Heat Transfer*, 9, 4, 686-693.

Tzou D. Y., 1995, The generalized lagging response in small-scale and high-rate heating, *International Journal of Heat and Mass Transfer*, 38, 17, 3231-3240.

Tzou D. Y., 1995, A Unified Field Approach for Heat Conduction From Macro- to Micro-Scales, *Journal of Heat Transfer*, 117, 1, 8-16.

Tzou D. Y., 2014, *Macro- to Microscale Heat Transfer: The Lagging Behavior*, pp. 25-56, Wiley Online Library.

Vernotte P., 1958, Les paradoxes de la theorie continue de l'equation de la chaleur, *Compt. Rendu*, 246, 3154-3155.

Yuvaraj R., and Senthil Kumar D., 2020, Numerical simulation of thermal wave propagation and collision in thin film using finite element solution, *Journal of Thermal Analysis and Calorimetry*, 142, 6, 2351-2369.

R. YUVARAJ is an Assistant Professor, Department of Mechanical Engineering, Sona College of Technology, Salem, Tamilnadu, India. He received his B.E. Mechanical Engineering degree from Government College of Engineering Salem, Periyar University, Salem, Tamilnadu, India, in the year 2004. He obtained his M.E. Thermal Engineering degree from Government College of Engineering Salem, Anna University, Chennai, Tamilnadu, India, in the year 2012. He has submitted his Ph.D thesis to Anna University, Chennai, Tamilnadu, India. His research focuses on macro-, micro- and nano-scale heat transfer, dropwise condensation, thin film preparation for superhydrophobicity, defrosting on superhydrophobic surface, droplet condensation modeling and simulations. He currently teaches "Applied Thermodynamics, Python Programming and Problem Solving" courses in Sona College of Technology, Salem, Tamilnadu, India.

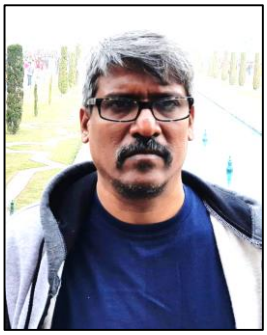

Dr. D. SENTHILKUMAR is a Professor and Head of Department of Mechanical Engineering, Sona College of Technology, Salem, Tamilnadu, India. He received his B.E. Mechanical Engineering degree from Annamalai University, Tamilnadu, India, in the year 1995. He obtained his M.E. Thermal Power Engineering degree from Annamalai University, Tamilnadu, India, in the year 1997. He obained his Ph.D degree from Indian Institute of Technology Roorkee, Uttrakhand, India. His research focuses on heat transfer, dropwise condensation, thin film preparation for superhydrophobicity, defrosting on superhydrophobic surface, pool boiling heat transfer, vaporization bio-fuel droplet, flow visualization, alternative fuels, double diffusive mixed convection, and moisture transport. He received grants from AICTE India, MHRD-ISTE India, and filed a Patent "A method surface texture of copper for the enhancement of dropwise condensation".